Modeling of Delamination Failure in Woven Fabric Reinforced Composites Under Mixed Mode Loading

Jawadullah

NUST201464468MCEME35114F

Supervisor

Dr. Hasan Aftab Saeed

DEPARTMENT OF MECHANICAL ENGINEERING

COLLEGE OF ELECTRICAL & MECHANICAL ENGINEERING

NATIONAL UNIVERSITY OF SCIENCES AND TECHNOLOGY

ISLAMABAD

November 2017

Modeling of Delamination Failure in Woven Fabric Reinforced Composites Under Mixed Mode Loading

Jawadullah

NUST201464468MCEME35114F

A thesis submitted in partial fulfillment of the requirements for the degree of

MS Mechanical Engineering

Thesis Supervisor:

Dr. Hasan Aftab Saeed

Thesis Supervisor's Signature: _____

DEPARTMENT OF MECHANICAL ENGINEERING

COLLEGE OF ELECTRICAL & MECHANICAL ENGINEERING

NATIONAL UNIVERSITY OF SCIENCES AND TECHNOLOGY,

ISLAMABAD

November 2017

Declaration

I certify that this research work titled "**modeling of delamination failure in woven fabric reinforced composites under mixed mode loading***"* is my own work. The work has not been presented elsewhere for assessment. The material that has been used from other sources it has been properly acknowledged / referred.

Signature of Student

Jawadullah

NUST201464468MCEME35114F

Language Correctness Certificate

This thesis has been read by an English expert and is free of typing, syntax, semantic, grammatical and spelling mistakes. Thesis is also according to the format given by the university.

Signature of Student

Jawadullah

NUST201464468MCEME35114F

Signature of Supervisor

Copyright Statement

Acknowledgements

I would like to thank everyone who has supported me since I began my graduate studies here at NUST. Your love, support and encouragement has made my experience here much more enjoyable and rewarding. Sometimes nothing seems to go in the right direction; you need to have patience and persistence, which would not have been possible without the support of my friends, family and loved ones.

First and foremost, I would also like to express special thanks to my supervisor Dr. Hasan Aftab for his help throughout my thesis. I admire his passion and dedication to his research and students. Dr. Rizwan Saeed Choudhry was the first person who introduced me to the field of woven fabric composites. He got me started on this research and pushed me to tackle some interesting problems. I would also like to pay special thanks to Dr. Raja Amir Azim and Dr. Sajid Ullah Butt for their support and service on my committee.

Finally, I thank my parents and brothers for their care and love. Your support and encouragement has been the backbone of my life. Thank you for always believing in me.

Jawadullah

College of E&ME, NUST

2017

Dedicated to my Parents and Brothers whose tremendous support and cooperation led me to this wonderful accomplishment

ABSTRACT

Woven fabric reinforced composites are used extensively in aerospace, automobile and wind turbine blades etc. Delamination is one of the most common type of damage in composite laminates due to their week interfacial strength. Delamination in composites is studied extensively in the past few years. Delamination can occur in different modes. Practically delamination occurs in mixed mode. Woven fabric reinforced composites exhibit complex failure mechanisms such as fiber cracking, matrix cracking and interface damage modes predominantly delamination. For prediction of delamination as a main concern, several modeling techniques has been suggested in literature which can be used to model the interface to predict the damage initiation and propagation of the interface.

This thesis focuses on numerical simulation of mixed mode woven fabric reinforced composite with experimental validation of the model. Comprehensive numerical model incorporating all the mixed mode ratios detailing progressive delamination and how to run mixed mode with high mesh densities have not been studied yet. Mixed mode experimental tests have been conducted with various mode ratios to obtain the load-displacement curves according to astm standard. Numerical model is suggested using the built-in composite layup model for plies and cohesive zone model is used for predicting the progressive damage of the interface. The validated model is then used to analyze different configuration of scarf joint.

Contents

LIST OF FIGURES

LIST OF TABLES

(This page intentionally left blank)

Chapter 1:

INTRODUCTION

1.1 Overview

Woven fabric reinforced composites are used extensively in aerospace, automobile and wind turbine blades etc. Delamination is one of the most common type of damage in composite laminates due to their week interfacial strength. Delamination in composites is studied extensively in the past few years. Woven fabric reinforced composites exhibit complex failure mechanisms such as fiber cracking, matrix cracking and interface damage modes predominantly delamination. Delamination can occur in different modes. Practically delamination occurs in mixed mode. A numerical model for accurately predicting the mixed mode delamination is required. A detailed orthotropic model with an interface modeled as cohesive zone elements to predict the delamination propagation is used in this thesis.

For prediction of delamination as a main concern, several modeling techniques has been suggested in literature which can be used to model the interface to predict the damage initiation and propagation of the interface [1, 2, 3, 4, 5, 6]. Most analyses of delamination apply a Virtual crack closure technique approach to model the interface which requires complex meshing techniques to advance the crack front, Other analyses use the fracture mechanics approach to evaluate the fracture energy through J-integral [1, 2]. A more advanced and appealing approach to overcome all the complexities is cohesive zone approach. Cohesive zone modeling was first suggested by Dugdale [4], and later Barenblatt [7] and Hillerborg et al [8] added improvements in it. Since after many authors have worked on cohesive zone approach [6, 9, 10].

For better performance of composite laminates, woven fabric reinforced composites are preferred over unidirectional laminates. Behavior of different unidirectional and multidirectional laminates subjected to mixed mode loading have been the focus of many researchers for the past years [11, 12, 13, 14, 15, 16]. The performance of composite laminates depends on stacking sequence, Fiber orientation, fiber matrix bonding and fracture toughness of the specimen subjected to delamination. Enhanced properties have been proved experimentally with different fiber orientations [12, 15].

This thesis focuses on numerical simulation of mixed mode woven fabric reinforced composite with experimental validation of the model. Comprehensive numerical model incorporating all the mixed mode ratios detailing progressive delamination and how to run mixed mode with high mesh densities have not been studied yet. Mixed mode experimental tests have been conducted with various mode ratios to obtain the load-displacement curves according to astm standard [17]. Numerical model is suggested using the built-in composite layup model for plies and cohesive zone model is used for predicting the progressive damage of the interface. The validated model is then used to analyze different configuration of scarf joint.

1.2 Applications of composite laminates

Composite laminates have wide range of application in automobile industry, aerospace industry, in wind turbine blades and other engineering structures. They are favored due to their high strength to weight ratios.

Military aircraft designers were among the first to realize the tremendous potential of composites with high specific strength and high specific stiffness since performance of those vehicles depends primarily on the weight. Composite usage also leads to smooth surfaces which reduce drag. Since boron and graphite fibers were developed in early 1960s, application of advanced composite in military aircrafts have been accelerated quickly. They bring typical weight savings of about 20%.

The NASA space shuttle has many composite parts that include graphite/epoxy cargo doors and experimental graphite/epoxy solid rockets. For large space structures such as the proposed space station the key properties of the structural materials are high stiffness to weight ratio, low thermal expansion coefficient and good vibration damping characteristics. In all these three areas composites offer significant advantage over conventional metallic materials.

Structural weight is also very important in automotive vehicles and the use of automotive vehicle components continues to grow. Glass fiber reinforced composites continue to dominate the automotive industry.

1.3 Aims and objectives

The main objective of this study is to propose a numerical cohesive zone model using fracture toughness data for determination of mixed mode delamination in composite laminates. Then validate the numerical model with experimental results. Then use the validated model for different configuration of scarf joint study and compare the results of those with analytical results of scarf joint. For validation of numerical model experimental data is required. The experimental data is taken from mixed mode bending tests that were previously performed by the advisor in his Phd thesis [18].

This study has two parts; one is proposing a numerical model and validating that numerical model with experimental data, and second one is the application part in which the validated model is used to analyze different configuration of scarf joint.

The substantial objectives to help this aim are:

- A detailed review to develop a comprehensive understanding of the work which has already been done for mixed mode bending test and scarf joints. This include a thorough grip on finite element modeling software (Abaqus) for modeling of the problem.
- Literature review to develop updated understanding of the numerical modeling techniques, damage initiation and progressive damage model used in analysis of composite laminates.
- Taking experimental data from the previous work and making force displacement graphs from that experimental data.
- Making numerical model and studying correct boundary conditions for the model.
- Running the numerical model for different mesh densities to obtain a mesh independent model, and cases for different velocity rates to study the effect of velocity rate.
- Creating model for different mode mix cases and running model for every case to obtain force displacement graphs.
- Comparing all the cases with the experimental mode mix cases; hence, validating the model.
- After validation, different scarf joint configuration is taken, and same validated model is used in those configurations.
- Failure load for different configurations of scarf joints is calculated and comparison of different configuration with each other is done.

1.4 Methodology of thesis

The overall methodology used in the thesis is given in the flow chart:

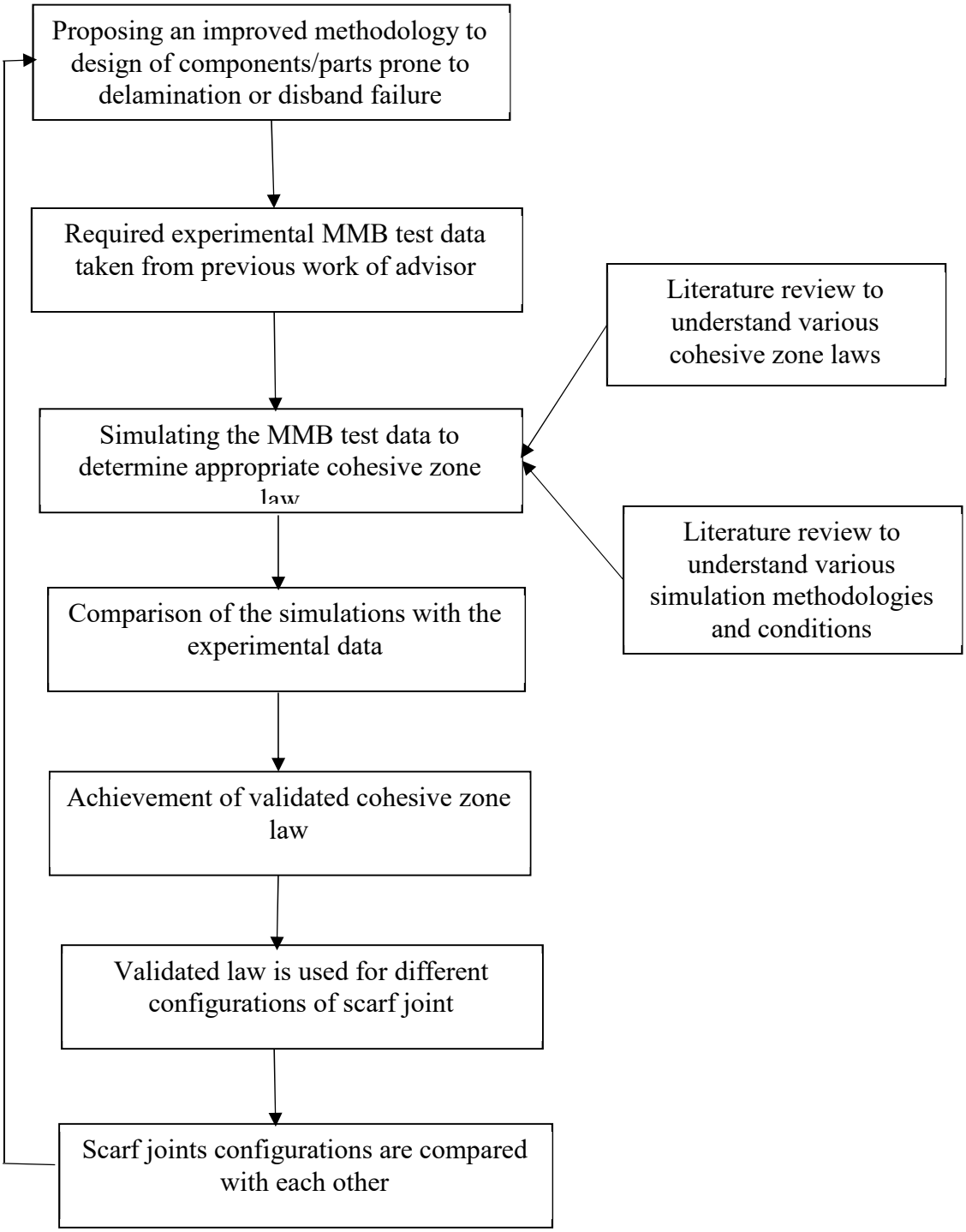

1.4.1 Summary of Methodology

First an extensive literature review was carried out to find the appropriate methodology for numerical modeling. Appropriate boundary conditions were studied and applied to the model. Mesh convergence study was carried out. Parametric study was carried out for the model. Different cases for five mode mix ratios were run and the force displacement plots were obtained. The force displacement graphs were compared with the experimental graphs and a validated model was obtained. The validated model was used to make different configurations of scarf joints. Failure load for different configurations of the scarf joints was calculated and compared with each other.

1.5 Contributions

- A fully validated model for cohesive zone approach is proposed in this thesis with application to different configuration of scarf joints.
- Although cohesive zone approach is available in literature but such an extensive study with validation of proposed cohesive zone model and applying that model on scarf joint is not available.

Chapter 2:

LITERATURE REVIEW

2.1 Delamination in composites

In this section, relevant work regarding experimentation and simulation of delamination in composites have been reviewed.

P. Naghipour et al. [19]

In this paper, a methodology for progressive damage simulation of unidirectional and multidirectional composite laminates has been represented using FE simulations, fracture experiments and analytical method. The laminates used were of carbon fiber reinforced polymer matrix composites. Numerical model is implemented in abaqus using bilinear elements subjected to mixed mode bending test and assembly of damageable layers. Numerical model is compared with experimental model and analytical results.

A. Turon et al. [20]

In this paper, a methodology for accurate prediction of delamination in composite laminates through cohesive zone has been devised. This paper shows that changes in local mode ratio can cause errors under mixed mode loading in determination of energy dissipation during evolution of damage. To tackle this issue relationships between interlaminar strength and penalty stiffness has been proposed. The proposed model has been compared with analytical results.

A. Turon et al. [21]

In this paper, a methodology that accounts for the constitutive behavior of progressive delamination has been proposed. The size and length of cohesive zone elements is the focus to anticipate correct dissipation of energy. Mesh size of the interface effects the damage progression in simulations. Guidelines for using appropriate element size is recommended in this paper.

L. Zhao et al. [22]

In this paper, a numerical model has been proposed for accurate simulation of mode 1 and mixed mode delamination propagation using cohesive zone elements. To anticipate progressive damage evolution, a fracture toughness function is used instead of constant fracture value. The numerical model is compared with the experimental findings.

P.P. Camanho et al. [23]

In this paper, a numerical model dealing with crack propagation is proposed with a new decohesion element under mixed mode loading condition. The element is used between solid finite elements to deal with initiation of damage and for propagation a single relative displacement parameter is used. Benzeggagh-kenane criteria (softening criteria) is used to deal with propagation of delamination. The results of the model are compared with experimental results.

N.E. Jansson et al. [24]

In this paper, for modelling delamination propagation an interface element has been proposed. Damage initiation of the model is evaluated from interlaminar fracture stresses whereas damage progression is calculated from mixed mode fracture toughness. The model is implemented in Finite element code.

M.L. Benzeggagh et al. [25]

In this paper, damage initiation and progressive damage of glass epoxy composite under mode I mode II and mixed mode I+II were evaluated. The concept of strain energy release rate and total fracture toughness is used. Mixed mode bending apparatus was used to perform the test. Experimental results were compared with semi-empirical criterion of plotting the critical strain energy release rate to the modal ratio.

S. Bennati et al. [26]

In this paper, a mechanical model of mixed mode bending test has been represented for interlaminar fracture toughness of composite laminates. An assembly of laminates connected by elastic-brittle interface represents composite laminates. The problem is evaluated through 36 differential equations and solved by considering separately symmetric and antisymmetric parts of loads.

M. Samimi et al. [27]

In this paper, a 2D cohesive zone model with enriched elements in fracture zone is used. A self-adaptive cohesive zone model is used to simulate large deformation. Irreversible traction separation law is used for delamination simulation and the model is developed for mode mix response of bi-material interfaces. The results are compared with experimental results.

A.E. Oskui et al. [28]

In this paper, a new loading device is introduced for mixed mode bending test. The disadvantages with the previous method loading device are addressed here. A 3D model of the new loading device is made to evaluate the values of stress intensity factor for mode I, mode II and mode III for comparison of results. ABS (acrylonitrile butadiene styrene) polymeric material was used for this study. Tests were also performed according to the previous method and both were compared.

C. Balzani et al. [29]

In this paper, a comparison between the linear softening material law and exponential softening law is carried out for cohesive zone model. This paper addresses the effects of softening after damage onset in the interface. By comparison of both the models, better convergence behavior is detected in the exponential material model.

A.B Pereira et al. [30]

In this paper, an experimental study has been taken on mode II fracture toughness of carbon/epoxy laminates. To define stacking sequences for the test a 3D study, finite element analysis was done. The level of mode-mixity, strain energy release rate and residual stresses were concluded from the FE analysis. Experimental results showed that mode II fracture toughness increases by increasing ply angle of the specimens. The results agreed with the interlaminar stress fracture criteria.

M.M. Shokrieh et al. [31]

In this paper, a new method for modeling delamination initiation and propagation is proposed for Double cantilevered beam (DCB). This model overcomes the issues that are with the crack closer technique and critical length method technique. Stiffness of the model is decreased in this method and this new method, in which critical length method is coupled with stiffness reduction, is called stiffness reduction-critical length method. The results obtained from this model agreed with the experimental results.

P.W. Harper et al. [32]

In this paper, a detailed study of the effect of the interface stress on the interface element has been carried out. The mode ratio, stress distribution and length effects on non-linear cohesive zone has been analyzed for damage onset on crack tip. The effects of input parameters with respect to modelling techniques have been analyzed especially in mode mix cases. Results from fracture mechanics analysis of strain energy release rate are compared with energy absorbed by interface elements. Initial tests are performed on standard fracture specimens and then ply drop specimens are modelled for other tests. Results are compared with crack closer technique. Results showed that modelling of complex geometries are sensitive to maximum interface stress.

B.R.K. Blackman et al. [33]

In this paper, A cohesive zone model is used for the analysis which is treated here as a two-parameter approach i.e. maximum stress and critical fracture toughness. The maximum stress or

strength of the model is the limiting value of stress ahead of the onset of damage and the critical fracture toughness is mainly concern with the damage onset of the model. The cohesive zone approach has been used with finite element analysis method. The finite element method results are compared with analytical method. The study reveals that cohesive zone modeling is best for fracture process.

2.1.1 Concluding Remarks

In all the above papers, Experimental methods of mixed mode bending tests are discussed for delamination failure and different methods were applied to numerically simulate the mixed mode bending test. Different damage initiation and progressive damage models were used. Cohesive zone approach was found best simulating model for mixed mode bending test. Mesh convergence study was applied in different papers.

Different Methods to simulate delamination failure in composites can be summarized as

1. The Virtual Crack Closure Technique for modeling delamination failure.
2. The Crack Closer and Critical Length technique.
3. Stiffness Reduction Critical- Critical Length method.
4. Cohesive Zone Modelling Technique.

In all these methods, different delamination initiation and damage softening approaches were used. In the review papers [19, 22], P. Naghipour et al and L. Zhao et al used Cohesive Zone approach for modeling mixed mode delamination failure. Linear Elastic models were used up till damage initiation. Maximum damage criteria were used for initiation of damage in the model and B-K Criteria with linear or exponential softening criteria was used for damage onset in the model. The models were simulated in Finite element analysis software. In Literature review it was concluded that Cohesive zone model was not used with woven fabric reinforced composites.

Model validation with cohesive zone approach for woven fabric reinforced composite is done in this thesis and validated model is used here for application in scarf joints.

2.2 Benchmark Case Study

Experimental tests of mixed mode bending have been done in the Phd work of R.S. Choudhry [34]. It is these experimental tests from where experimental data has been taken for this thesis. Experimental data has been taken and numerically simulated model has been validated with these experimental tests. This study has three phases, Experimental tests, Numerical simulation, validation and the third one is application of the model in scarf joints.

Experimental data is taken, and other two phases are done in this thesis.

Details of the Experimental data is discussed here.

2.2.1 Model Geometry

Figure (2.1) shows the model geometry and figure (2.2) shows schematic of the model.

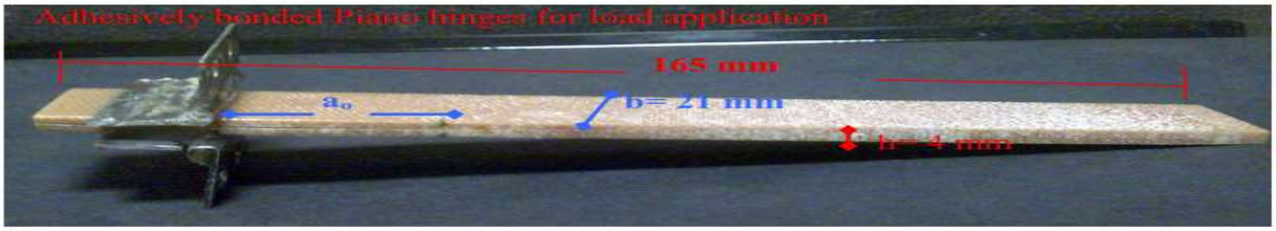

Figure 2. 1 Split laminate specimen for MMB test (a_0 is initial delamination length) *[34]*

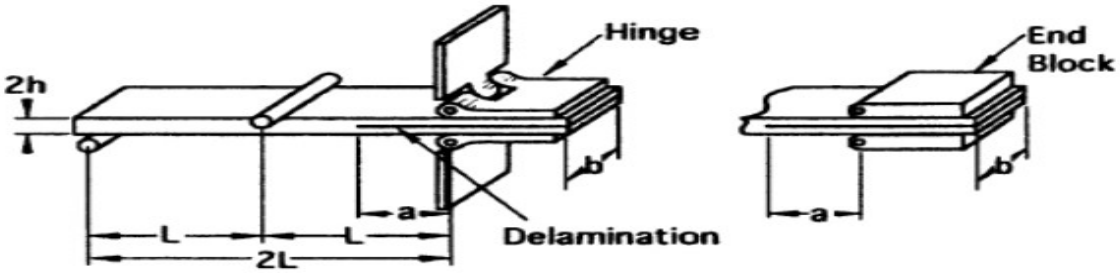

Figure 2. 2 Schematic representation of MMB test specimen *[35]*

2.2.2 Specimen Details

Specimens for experimental tests were prepared using Primco-SL246/40, which is glass fiber/phenolic pre-preg. (8-harness stin weave glass fabric pre-impregnated with a modified phenolic resin mix to a nominal 40% resin content). Quick step method was used to manufacture

these specimens. The layup consists of 12 layers of prepreg ($0/0_f$). A polymer film with thickness between 5-7μm was used as delamination insert after laying up six plies. The delamination insert length was approximately 65mm (to have approximately 50mm of delamination after cutting the edges). The final approximate dimension of the specimens were, span length 110mm, width 20mm, thickness 4mm and delamination length 30mm.

2.2.3 Experimental procedure

Reeder and Crews [36, 37] first proposed mixed mode bending test. This standard after improvements and redesign has been adopted by American Society for Testing Materials as ASTM D6671/D6671 M-03 [35]. This standard is followed for experimental work. This test method is commonly referred as Mixed Mode Bending (MMB) test. Standard test fixture required for these tests was supplied by Wyoming Test Fixtures, Inc. The MMB test fixture used in one of the tests with key components labeled, as shown in figure (2.3).

Initiation and progressive damage of delamination in composite laminates take place under combined effect of normal and shear mode. The MMB loading is combination of simple mode 1 (Normal) and mode 2 (Shear). Figure (2.3) shows the picture of the actual test, the load P applied and the loading lever in terms of load P. The loading position c in figure (2.3) determines the mode mix that is applied.

Experimental tests were performed according to the standard [35]. Tests were performed for mode mix ratio of (20%, 30%, 50%,75% and 100%). Five specimens were tested for each mode mix ratio. Table 1 shows the different mode mix ratios and their corresponding loading lever positions. Mode mix ratio can be changed by changing the load position c. Pure mode 2 can be achieved by applying the load on the mid position of the specimen and pure mode 1 can be attained without lever by directly applying load on the hinge.

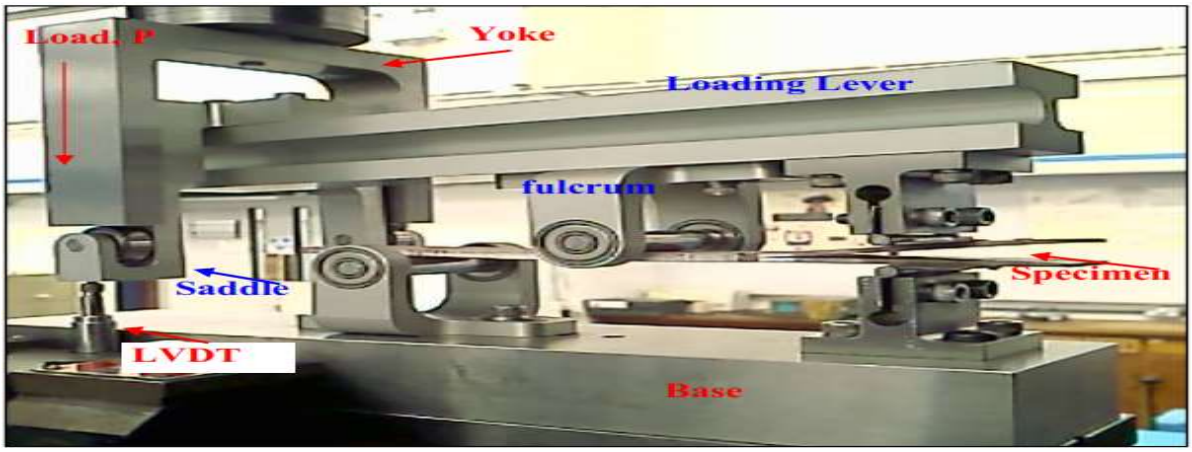

Figure 2. 3 Schematic representation of MMB test specimen *[34]*

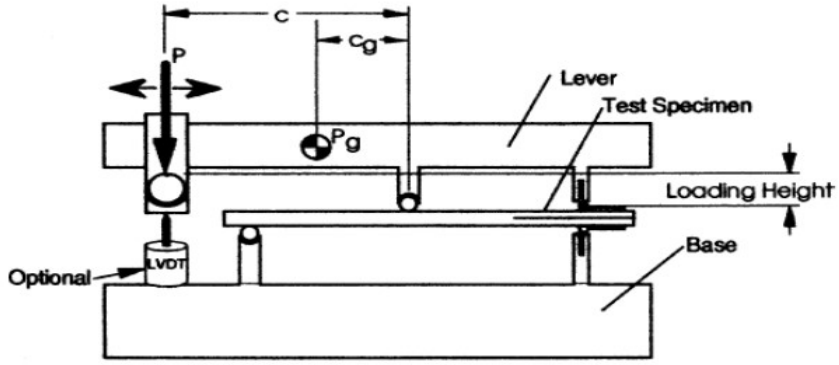

Figure 2. 4 The schematic of MMB apparatus *[35]*

Table 2. 1 Mode mix ratio and loading lever

Mode mix	20%	30%	50%	75%	100%
Loading lever c	112mm	67mm	39mm	29mm	21mm

Chapter 3:

METHODOLOGY

3.1 Improved methodology

Improved methodology for designing the components prone to delamination is proposed in this thesis. For this purpose, Numerical model is created through Abaqus software and numerical simulations are run. The numerical model data is compared with experimental data and a validated model is obtained. The experimental data is taken from the PhD thesis of R.S. Choudhry [18]. The validated model is then used in application to scarf joint FE analysis.

3.2 Numerical model

Numerical model is created in Abaqus software

3.2.1 Model details

The dimensions of the numerical model are same as the experimental model with span length of 110mm, width 20mm and thickness 4mm. Figure (3.1) shows the schematic of the model specimen. The 30mm length shows the initial delamination length in the specimen.

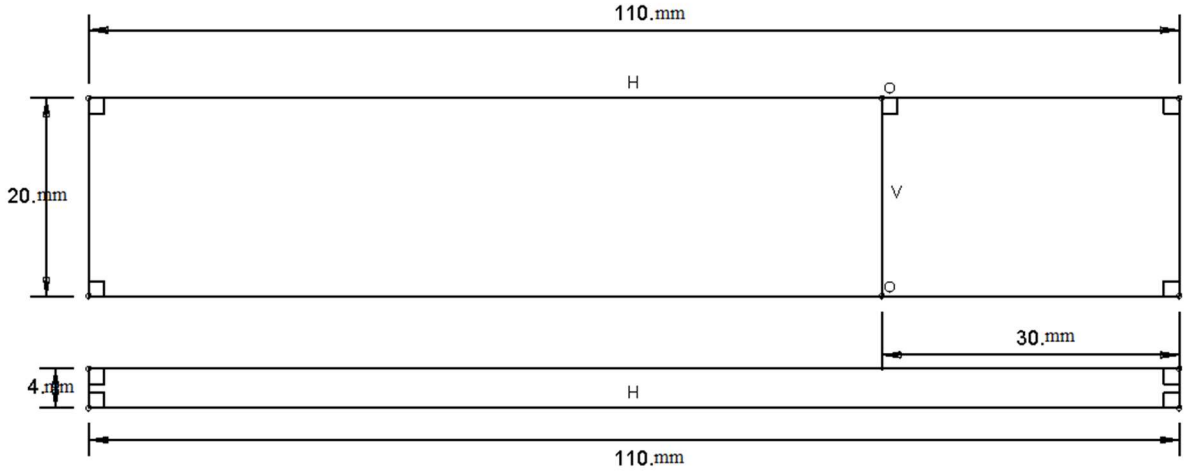

Figure 3. 1 Schematic of specimen dimensions

3.2.2 Boundary Conditions

Figure (3.2) shows the model boundary conditions. The boundary conditions were set accordingly with the experimental setup.

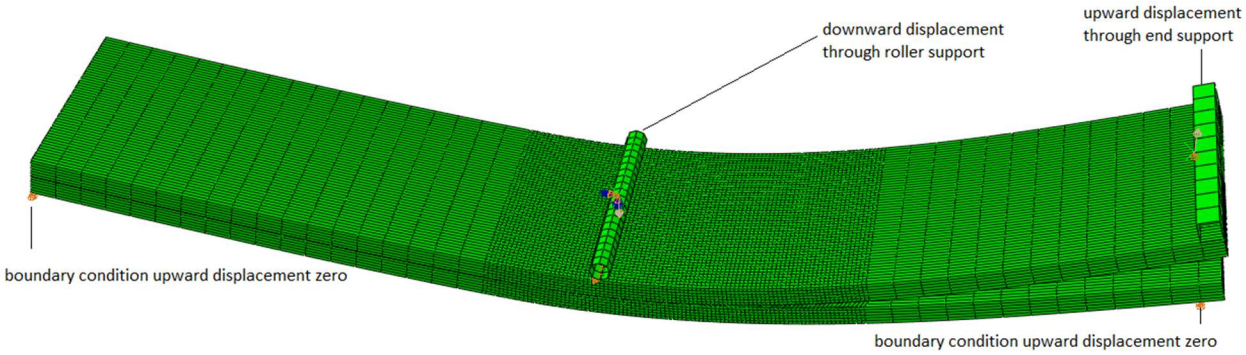

Figure 3. 2 Schematic of numerical model

The end support on upper side which is the hinge (for application of load in the experimental setup), was modeled as discrete rigid in FE model. The end support is linked with specimen as tie constraint and a dummy node is attached with this link. The load is applied as a displacement on this dummy node. To achieve different mode mix (G_{11}/G_t ratio) displacement boundary condition was applied according to equation given below.

$$U = (c + L)/L \times U_d + c/L \times U_u$$

Where U is the applied on the load point as displacement which is applied here through mid-point on roller support as U_u downward and hinge point U_u upward.

This equation was validated by discrete rigid link in one simulation, and by comparing the results of the two different mode mix ratios with the experimental results. The roller which works as a fulcrum in the experimental setup is designed here as discrete element roller and is placed on the specimen with general contact interaction defined. All degrees of freedom except z axis are given values of zero for this roller because this can only move in z axis. On the lower side of the specimen displacement in z axis is zero at two ends of the specimen which in experimental setup is achieved by roller supports holding the specimen.

3.2.3 Mesh details

Plies of the specimen are modeled through built-in composite layup of 12 layers and elements used are continuum shell elements with reduced integration (SC8R), Each layer was made of one continuum shell element and was found enough for mesh convergence.

The interface was inserted after six layers in the model. This is modeled as cohesive zone elements (COH3D8). The cohesive zone was generated through offset mesh. The initial delamination length was obtained by deleting mesh of the cohesive zone elements in mid plane of the specimen where required. Increased mesh density is used in specified portion of the specimen, from start area of the interface up to 20 mm away from the middle point where the fulcrum is attached to the specimen as shown in the figure (3.2). This was found best for fetching the correct response in the interface.

3.2.4 Material Modeling

(i) Individual plies model

Material type Lamina, which is built-in transversely isotropic plane stress material model (orthotropic), was used for the plies. It is based on the following equations [18].

$$6_{11} = Q_{11}.\varepsilon_1 + Q_{12}.\varepsilon_2 \qquad \tau_{12}=G_{12}\,\gamma_{12} \quad \text{for} \quad \tau_{12} \leq \tau_{nl}$$

$$6_{22} = Q_{21}.\varepsilon_1 + Q_{22}.\varepsilon_2 \qquad \tau_{12}=\tau_{nl}+G_{12}^{nl}.\,\Delta\,\gamma_{12} \quad \text{for} \quad \tau_{12} > \tau_{nl}$$

$$Q_{11} = \frac{E_1}{1 - v_{12}.v_{21}}$$

$$Q_{22} = \frac{E_2}{1 - v_{12}.v_{21}}$$

$$Q_{21} = Q_{12}$$

$$v_{21} = \frac{E_2}{E_1}.v_{12}$$

In the above equations σ_1 and ϵ_1 are normal stresses and strains in x- direction, σ_2 and ϵ_2 are stresses and strains in y direction. τ_{12} and γ_{12} are shear stress and shear strain in x-y plane. The

properties are given in table (3.1). The material was implemented in Abaqus through build in continuum shell elements excluding the interface model.

Table 3. 1 Properties of material for individual plies in numerical simulation *[18]*

ρ	Composite density	1566.3 kg $\mathbf{m^{-3}}$
E_1	Modulus of tensile in first direction	24.2 GPa
E_2	Modulus of tensile in second direction	23.1 GPa
υ_{12}	Poison's ratio	0.2
G_{12}	In-plane shear modulus	3.85 Gpa
E_3	Out of plane section modulus	7.71Gpa
K_{11}=K_{22}	Transverse shear stiffness of shell section in 13 and 23 planes	.428Mpa

(ii) Cohesive zone elements

After six layers, a layer of 3μm Cohesive zone elements was inserted for modeling the interface in the specimen. Cohesive zone is a special group of elements for modeling interfaces in Abaqus, when integrity of the bond is the interest in analysis. It is incorporated in the model to analyze delamination fronts and its location, and the extent to which delamination has occurred.

(iii) Traction Separation law

Three approaches are used for definition of cohesive zone elements; Traction-separation law, constitutive behavior and continuum behavior. For very thin interface as used in the model traction separation behavior is ideal.

In traction separation law [38], there is direct relationship between traction defined by τ_i at the interface and separation i.e. relative displacement defined by δ_i. The constitutive thickness is kept one in this model irrespective of the geometrical thickness. The microscopic based response can be ignored due to small thickness of the interface. The traction and displacement stiffness matrix is thus defined by penalty stiffness as defined below.

$K_I^0 = K_I \,.\, T_I^c$

Where

K_I^0 = Penalty stiffness Value

$K_I > IE5$ *and* $K_I < IE7$

T_I^c = (i = 1,2,3) are interlaminar tensile and shear strengths, in first and second direction respectively.

(iv) Damage Initiation

In cohesive zone, interface damage occurs in two steps; first one is damage initiation and second one is damage evolution. Damage initiation will start in the interface when certain damage criteria is met in the damage process. In Abaqus there are certain criteria defined for initiation of damage for cohesive interface elements. The best criteria that meet the results and predict correct response is Quadratic Nominal stress criteria symbolized in Abaqus as QUADS [39].

$$\left(\frac{\tau_n}{\tau_n^0}\right)^2 + \left(\frac{\tau_s}{\tau_s^0}\right)^2 + \left(\frac{\tau_t}{\tau_t^0}\right)^2 = 1$$

τ_n, τ_s, and τ_t are normal and shear elastic limits for the interface. Damage initiates as this criterion is met.

(v) Damage Evolution

After the damage initiates, damage evolution takes place. Damage evolution law is defined for damage propagation. Damage evolution model requires damage evolution law. Damage evolution law predicts and defines the onset of damage in the model.

A scalar damage parameter (D) defines damage evolution in traction separation law. It defines damage from 0 to 1. 0 means damage evolution hasn't started and 1 means complete damage has occurred. This damage parameter combines all active damages.

Traction can be defined with this damage parameter as

$$\tau_1 = (1 - D) . \overline{\tau_1} \qquad \text{for} \qquad \overline{\tau_1} \geq 0$$

$$\tau_2 = (1 - D) . \overline{\tau_2}$$

$$\tau_3 = (1 - D) . \overline{\tau_3}$$

In the above formulation, pure compression deformation doesnot initiate damage in the model, i.e compressive stiffness of the interface will not be degraded.

Many damage evolution laws are defined. Damage evolution laws can be applied in abaqus as power law, tabular law and benzeggagh-kenane criteria (BK). The one used in this modeling is B-K criteria

(vi) Benzeggagh – Kenane Criteria

The evolution of damage in the interface depends upon the mode mix condition or mode mix definition, as defined either by fracture energy or displacements. In this modeling the mode mix is defined in terms of fracture energy using B-K criteria which incorporates relative portions of normal and shear deformation.

Mode mix loading condition can be a combination of either of the three loading conditions. Those loading conditions are given in figure (3.3).

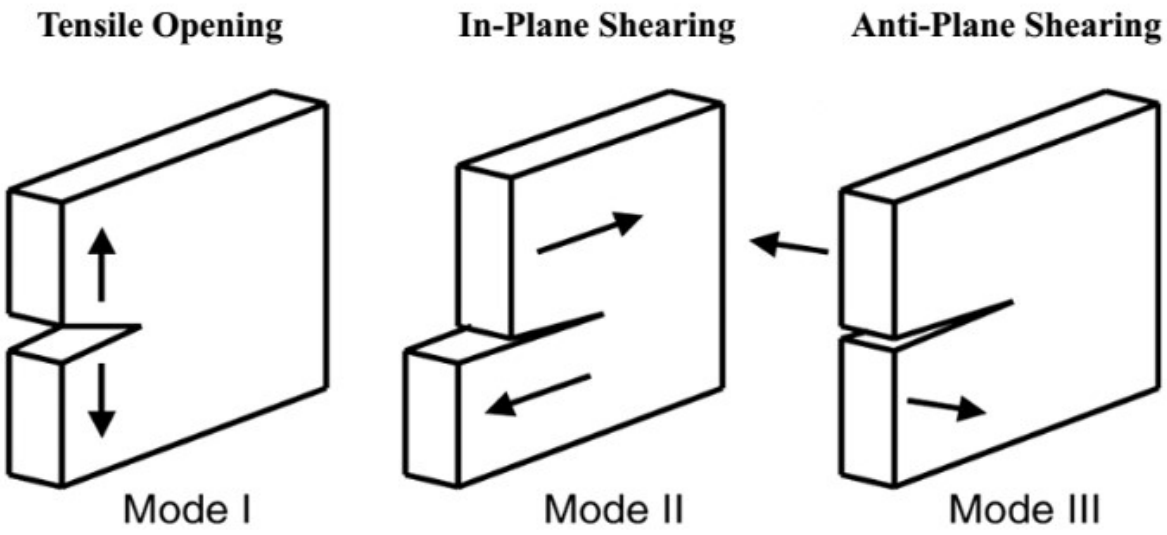

Figure 3. 3 Modes of loading

This criteria is combination of two modes i.e mode I and II. Mode III fracture energy is not known it is assumed equal to mode II fracture energy. This criteria can be expressed as

$$G^c = G_n^c + \{ (G_s^c - G_n^c) . (\frac{G_s}{G_T})^2$$

Where;

G^c = Mode mix fracture energy

G_n^c and G_s^c are critical fracture energies in normal and first shear direction.

$$G_s = G_s + G_T$$

n = material parameter

The whole material model for the interface is given in table (3.2)

Table 3. 2 Properties of material for cohesive zone *[18]*

ρ	Resin density	1085 kg m^{-3}
$K_{nn}=K_I^0$	Mode I penalty stiffness	44400 GPa
$K_{ss}=K_{II}^0$	Mode II penalty stiffness	22200 GPa
$K_{nn}=K_{III}^0$	Mode III penalty stiffness	22200 GPa
T_I^c	Inter-laminar tensile strength	44.4 MPa
$T_{II}^c=T_{III}^c$	Inter-laminar shear strength	22.2 MPa
G_{Ic}	Fracture Toughness in mode I	425 J m^{-2}
G_{Ic}	Fracture Toughness in mode II	905 J m^{-2}
η	Neta for progressive damage	4.8
	Softening	Linear

3.3 Model Validation

Numerical FE models are Simulated for all the experimental cases as given in table (3.3) FE models are created and simulated according to loading conditions. First mesh convergence has been studied taking case 2 in consideration. Effect of input displacement (loading speed) is also checked on case 2. Mass scaling is used in the FE simulations and its effect is also studied.

Figure 3. 4 Mode mix cases for FEA simulations

	Case 1	**Case 2**	**Case 3**	**Case 4**	**Case 5**
Mode mix cases	**20%**	**30%**	**50%**	**75%**	**100%**
Loading lever c	112mm	67mm	39mm	29mm	21mm

Load displacement data is obtained from the simulation of all the cases. The load displacement graphs are then compared with the experimental load displacement graph and model validation is done

3.4 Application to scarf joints

After validation of the model the model is applied on a scarf joint. The dimensions for the scarf joint is taken from D. Tzetis and P. J. Hogg paper [40]. The validated model for cohesive zone is used in this scarf joint analysis. The scarf joint is checked for different angles of scarfs. Detailed modeling is discussed in last chapter of the thesis

Chapter 4:

RESULTS AND VALIDATION

4.1 FE Simulation cases

After the modeling step of mixed mode bending test five cases were simulated for validation purpose. From simulation of the cases load displacement graphs were obtained and were compared with the experimental load displacement graphs. The details of the five cases is given in table (4.1). From these cases, case 2 was selected for mesh convergence study. Rate of displacement effect was also studied on case 2. Mass scaling was done to reduce our simulation cost and its effect was also studied on case 2.

Table 4. 1 FE simulation cases

	Case 1	**Case 2**	**Case 3**	**Case 4**	**Case 5**
Mode mix cases	**20%**	**30%**	**50%**	**75%**	**100%**
Loading lever c	112mm	67mm	39mm	29mm	21mm

4.2 Mesh Convergence study

Case 2 was selected for mesh convergence. Case 2 is 30 % mode mix case. The 30% mode mix was obtained by loading lever 67mm in experimental test, which is obtained here by applying the load displacement equation defined in previous chapter.

Six different mesh cases were studied. The mesh was refined in a specified area of interest which effects the results extensively, as shown in figure (4.1) where mesh density is high.

Six different mesh density cases were studied. The details of cases for mesh size in specified area is given in table (4.2). First two cases m1 and m2 were simulated with two layers in thickness direction. The other four cases i.e. m3, m4, m5 and m6 were simulated with 12 layers in thickness direction.

Graphs for cases m1 and m2 are given in figure (4.2), for case m3 and m4 are give in figure (4.3) and for case m5 and m6 are given in figure (4.4).

All the cases show similarity with experimental results in elastic portion, but damage progressive region does not meet with low mesh density. As mesh density is increased the graph show similarity even in damage progressive region.

Figure (4.5) shows graph between the load at which first failure start and number of elements in the specimen i.e. mesh density. This graph predicts that mesh convergence has been obtained, as no obvious change in the failure load occurs with further mesh size reduction or increasing number of elements.

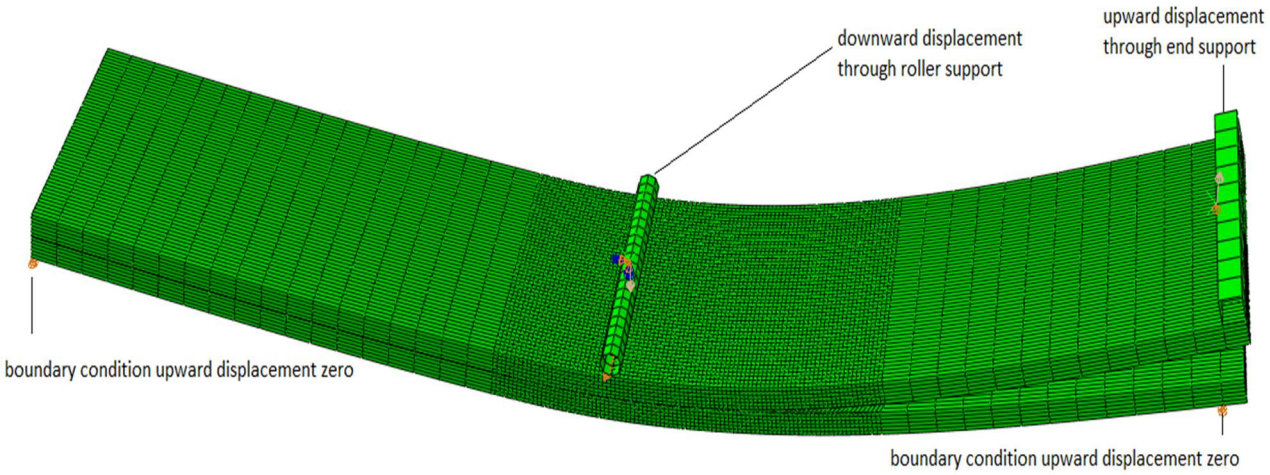

Figure 4. 1 schematic of FE specimen showing details of mesh density

Table 4. 2 Cases for mesh convergence

Case 2 sub cases	Case m1	Case m2	Case m3	Case m4	Case m5	Case m6
Mesh details	2.5mm/ 2 layers	1.5mm/ 2 layers	2.5mm/ 12 layers	1.25mm/ 12 layers	0.8mm/ 12 layers	0.4mm/ 12 layers

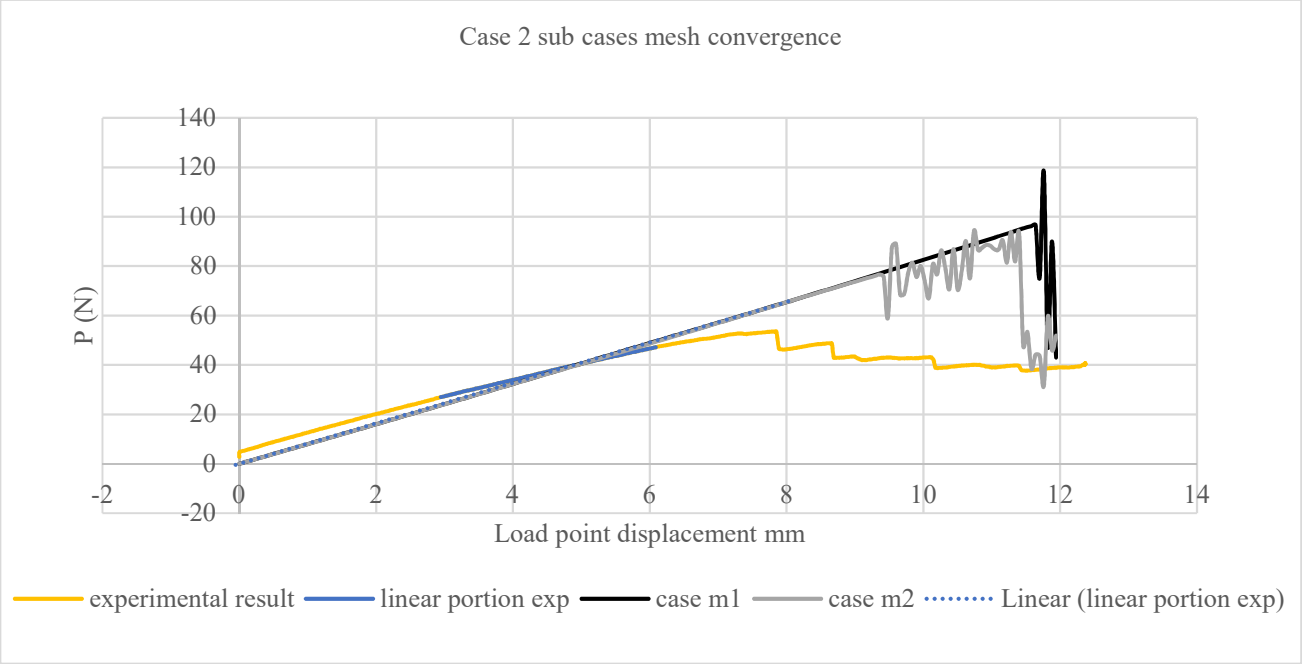

Figure 4. 2 Mesh convergence cases m1 and m2

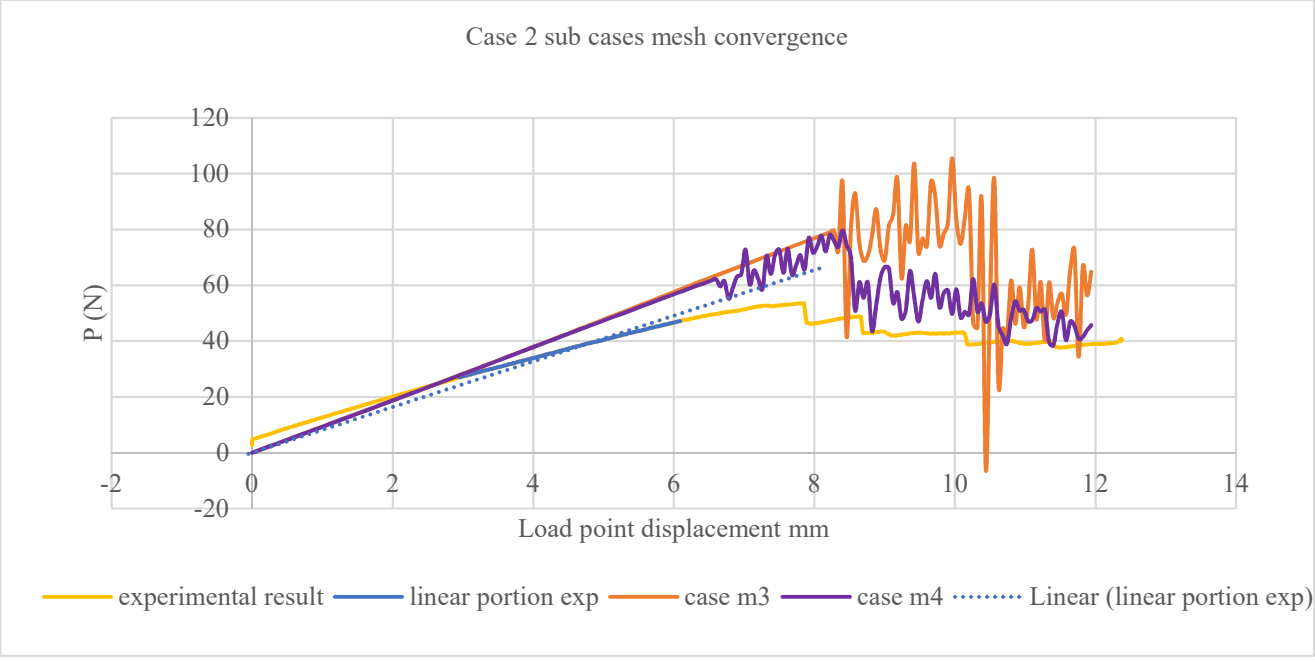

Figure 4. 3 Mesh convergence cases m3 and m4

Figure 4. 4 Mesh convergence cases m5 and m6

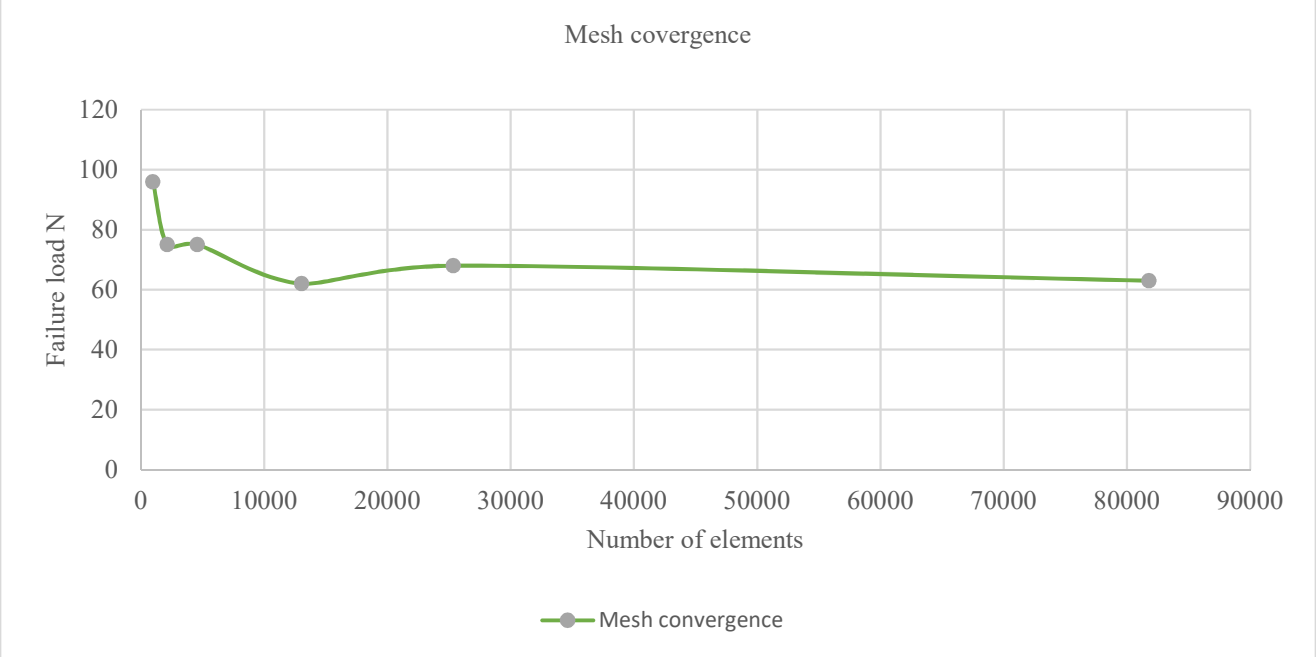

Figure 4. 5 Mesh convergence graph load versus mesh density

4.3 Effect of Displacement rate

Load is applied through displacement in FE simulation. The effect of rate of displacement was studied on case 2 i.e. mode mix ratio 30%. Three different displacement rate cases were simulated, i.e. case with velocity 1.5mm/s, case with velocity 3mm/s and with 6mm/s. The different displacement rates were applied through the displacement rate equation discussed in last chapter. The graphs are shown in figure (4.6). The converged mesh was used for all the cases.

The graphs overlap each other. This shows that our FE simulation does not depend on displacement rate at these values. We selected displacement rate of 6mm/s for further simulations.

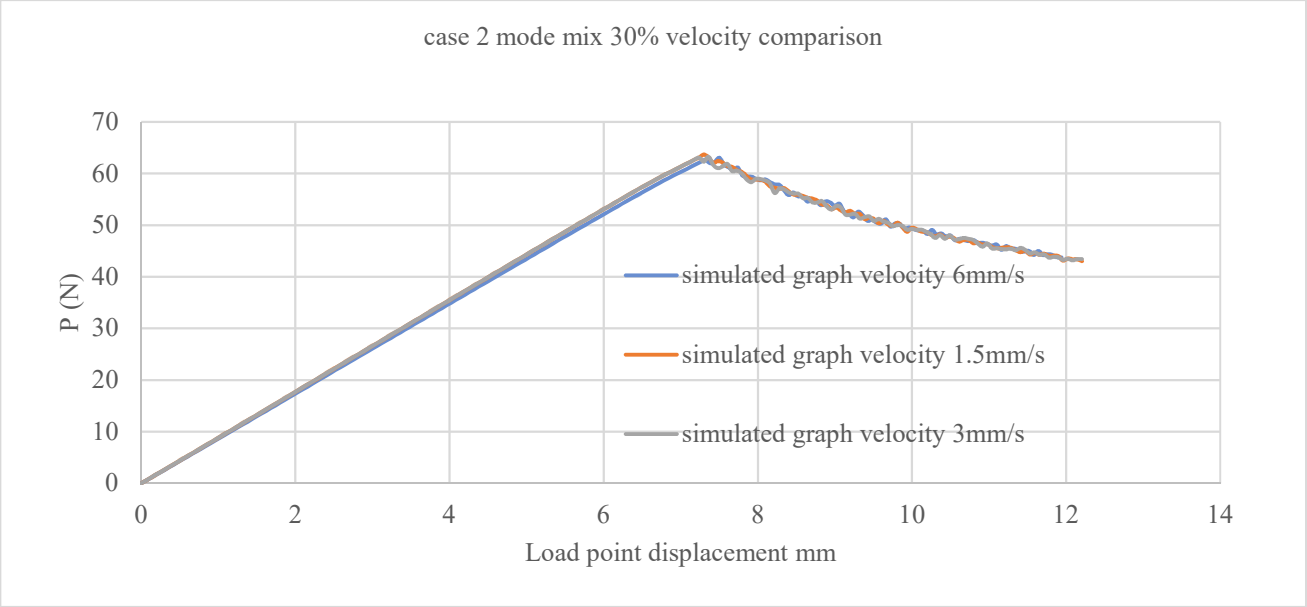

Figure 4. 6 displacement rate comparison

4.4 Mass Scaling Effect

To reduce the cost of Simulation, i.e. the simulation to execute faster mass scaling was applied on the cases. The effect of mass scaling on the results was studied for one case i.e. case 2. Two mass scaling cases are simulated for case 2, one is s1 and the other is s2 as shown in figure (4.7)

Case s1 is simulated at mass scaling of 10^-6 and case s2 at mass scaling of 10^-5. Mass scaling can result ripples in the results. We should find the mass scaling value that does not produce any ripples in the results. From the figure (4.7) it is shown that case s1 there are no ripples in the results with mass scaling of 10^-6 for our simulations. Mass scaling higher that this value show ripples in the results as shown by case s2 with mass scaling of 10^-5. So, we select mass scaling of 10^-6 for our simulations because no ripples are found in the graph for this mass scaling.

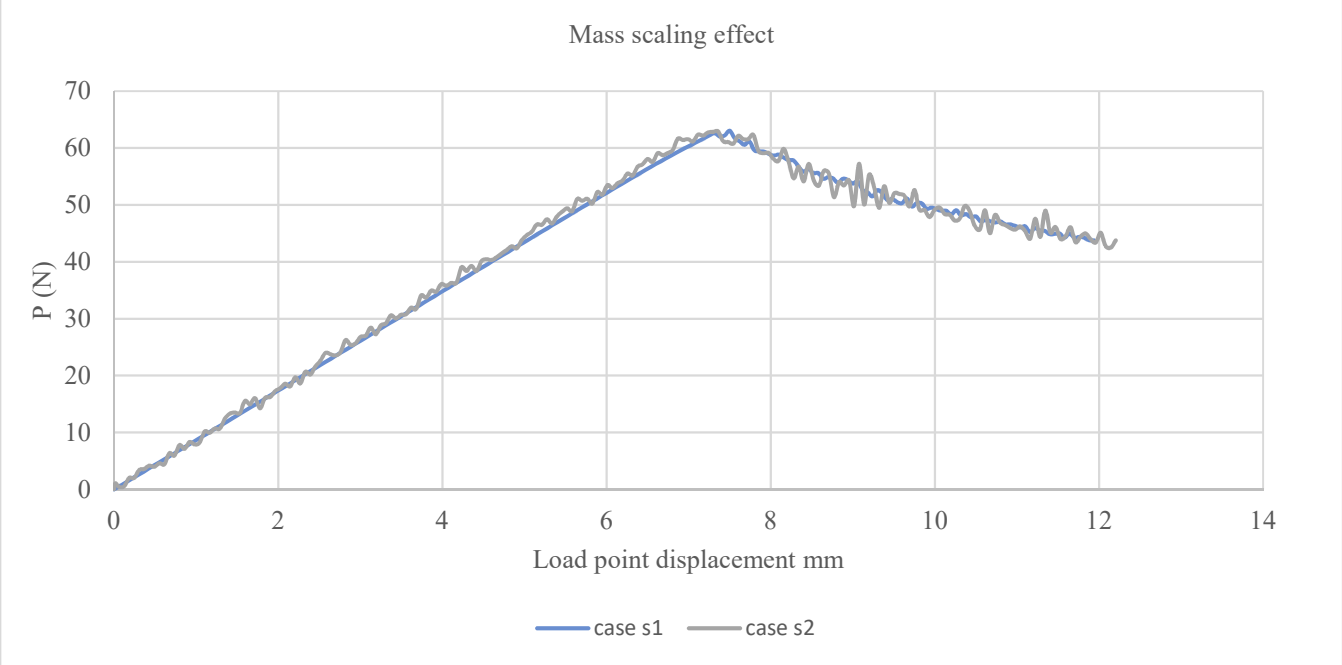

Figure 4. 7 load displacement graphs comparing mass scaling

4.5 Validation of the model

All five cases of mode mix were simulated, and results were obtained as load displacement graphs. These load displacement graphs were compared with the experimental graphs. Detail of every case is given below

4.5.1 Case 1

Case 1 is 20% mode mix case (i.e. 20% mode II and 80% mode I). The loading lever in experimental setup for this case was 112mm. This case is run at 6mm/s displacement rate. The mesh details are, total number of elements is 81996 in which 200 are rigid elements, 76128 are continuum shell elements and 5668 are cohesive zone elements. The case was run with mass scaling of 10^-6. The load displacement graph compared with experimental graph is given in Figure (4.8). The load is in Newton and the displacement is in millimeters.

In figure (4.8) one graph shows the experimental results and the other one shows the results from FE simulation. A linear portion is shown on the experimental graph as following the method from standard [17]. From this linear portion linear line is drawn for the experimental graph, shown as dotted line and named as linear experimental portion.

The linear experimental graph is compared with the FE simulation graph. This experimental graph and the FE simulation graph shows similar behavior. The Drop in the FE graph and the experimental shows the onset of damage. The onset of damage portion in the experimental graph and the FE simulated graph also shows approximately similar behavior.

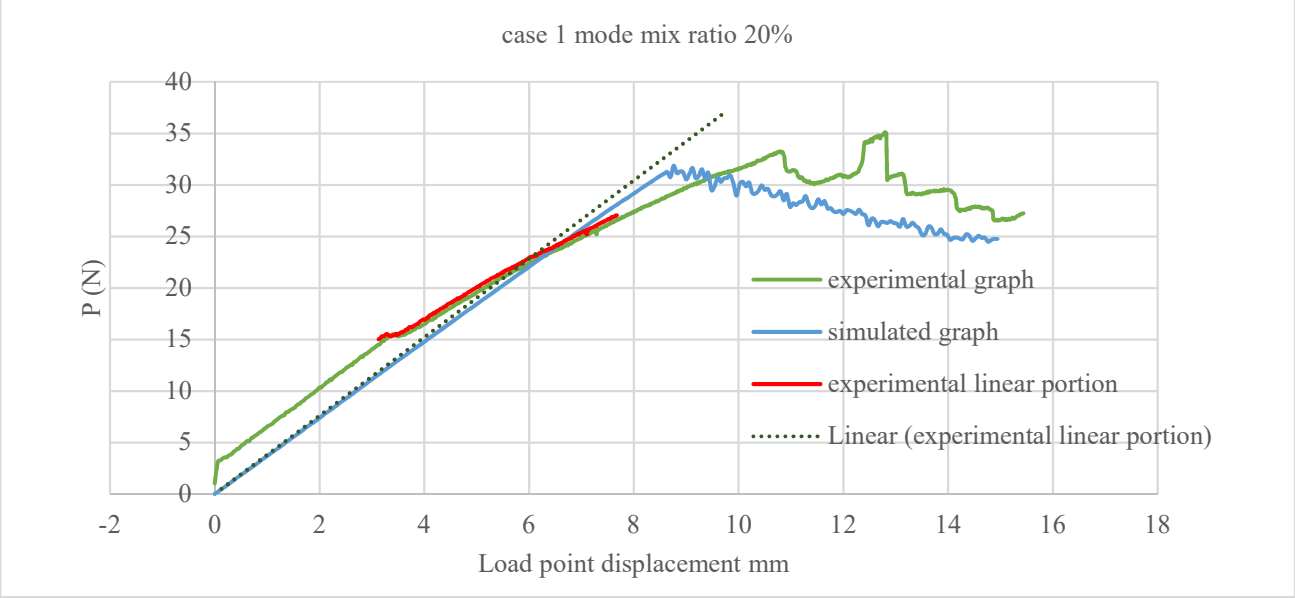

Figure 4. 8 Load displacement graph of case 1

4.5.2 Case 2

Case 2 is 30% mode mix case (i.e. 30% mode II and 70 % mode I). This is also mode I dominant case as the previous case. The loading lever in the experimental case for this mode mix was 67mm. This mode mix was obtained by the displacement equation. The case is run at a velocity of 6mm/s. Mass scaling of 10^-6 was applied in the case. The same mesh details were used for this case as the previous case. The load displacement graph from FE simulation of this case compared with experimental result is shown in Figure (4.9).

The linear portion of the experimental graph shows similar behavior with the FE results obtained. The onset of damage portion in the FE simulated graph also shows approximately similar behavior with the experimental graph.

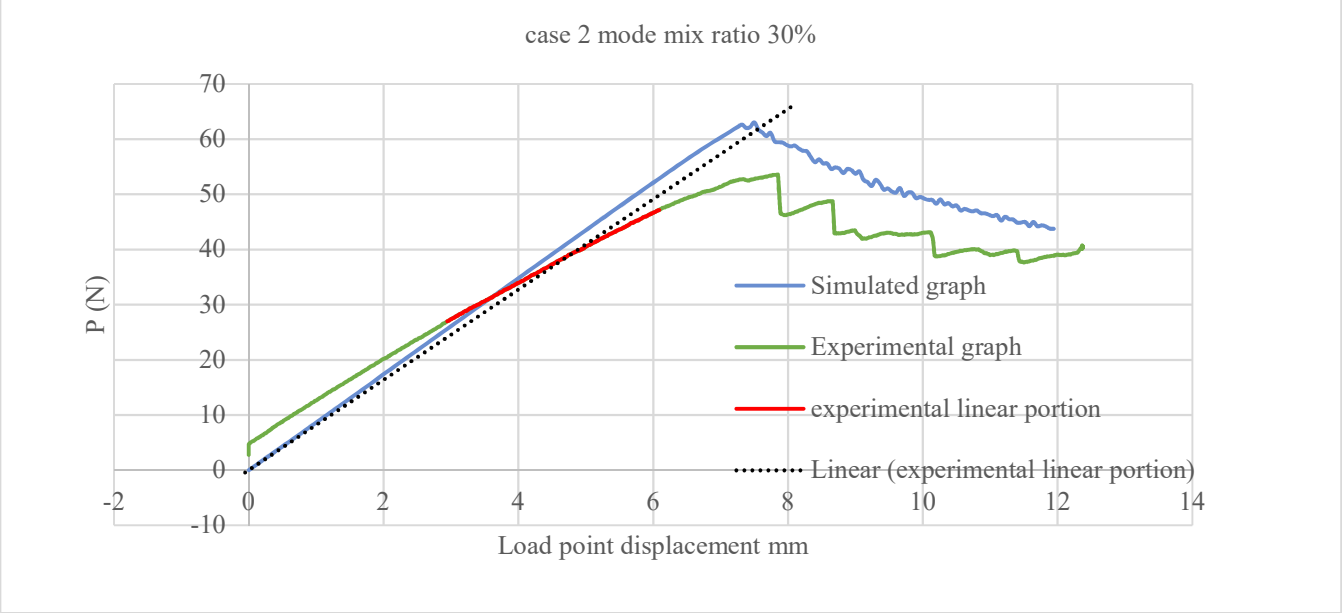

Figure 4. 9 Load displacement graph of case 2

4.5.3 Case 3

Case 3 is 50% mode mix case (i.e. 50% is mode I and 50% is mode II). The loading lever to obtain this mode mix in experimental case was 39 mm. In FE simulation, this mode mix was obtained by the displacement equation. The mesh details are same as the previous cases. This case was also run

at 6mm/s loading rate. The mass scaling in this case was also 10^-6. The FE load displacement graph compared with the experimental load displacement graph is shown in figure (4.10).

The linear portion of the experimental graph shows similar behavior with the FE results obtained. The onset of damage portion in the FE simulated graph also shows approximately similar behavior with the experimental graph.

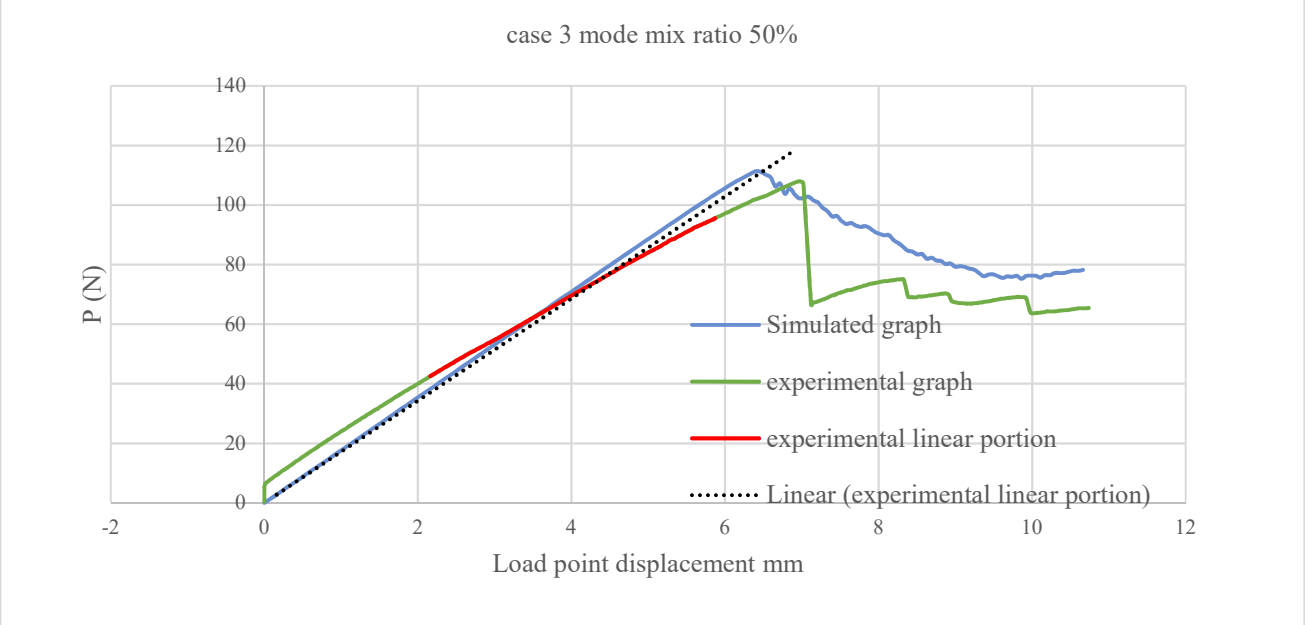

Figure 4. 10 Load displacement graph of case 3

4.5.4 Case 4

Case 4 is 75% mode mix case (i.e. 75% mode II and 25% mode I). In experimental setup to obtain this mode mix loading lever 29mm was applied. In FE simulation, this mode mix was obtained by displacement equation. The mesh details are same as the previous cases. The loading rate applied as displacement rate was 6mm/s. The case was run with a mass scaling of 10^-6. The FE load displacement graph compared with the experimental load displacement graph is shown in figure (4.11).

The linear portion of the experimental graph shows similar behavior with the FE results obtained. The onset of damage portion in the FE simulated graph also shows approximately similar behavior with the experimental graph. In cases where mode I is dominant onset of damage graph is more like experimental graphs than this case where mode II is dominant.

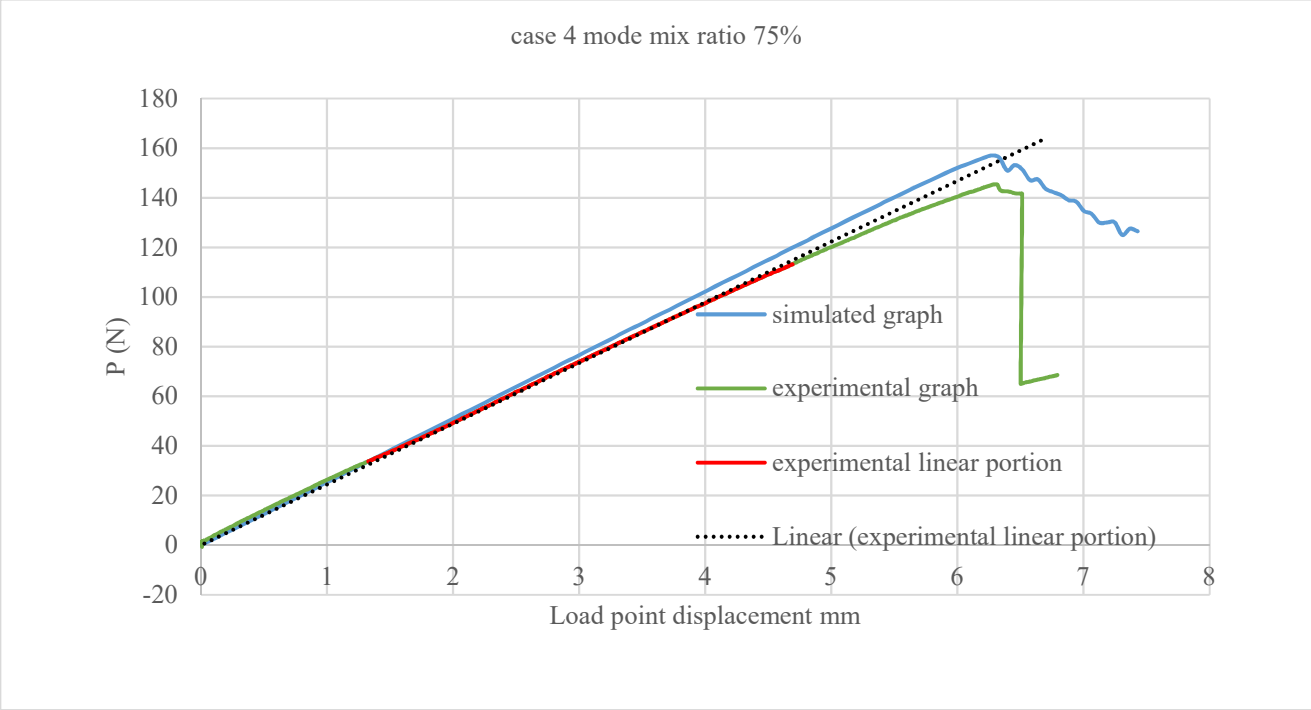

Figure 4. 11 Load displacement graph of case 4

4.5.5 Case 5

Case 5 is approximately 100% mode mix case (i.e. approximately mode II). In experimental setup to obtain this mode mix loading lever 21mm was applied. In FE simulation, this mode mix was obtained by displacement equation. The mesh details are same as the previous cases. The loading rate applied as displacement rate was 6mm/s. The case was run with a mass scaling of 10^-6. The FE load displacement graph compared with the experimental load displacement graph is shown in figure (4.12).

The linear portion of the experimental graph shows similar behavior with the FE results obtained. The onset of damage portion in the FE simulated graph also shows approximately similar behavior with the experimental graph. This is approximately pure mode II the onset of damage graph in FE simulation does not fully agree with the experimental data, but the trend is same in both the graphs.

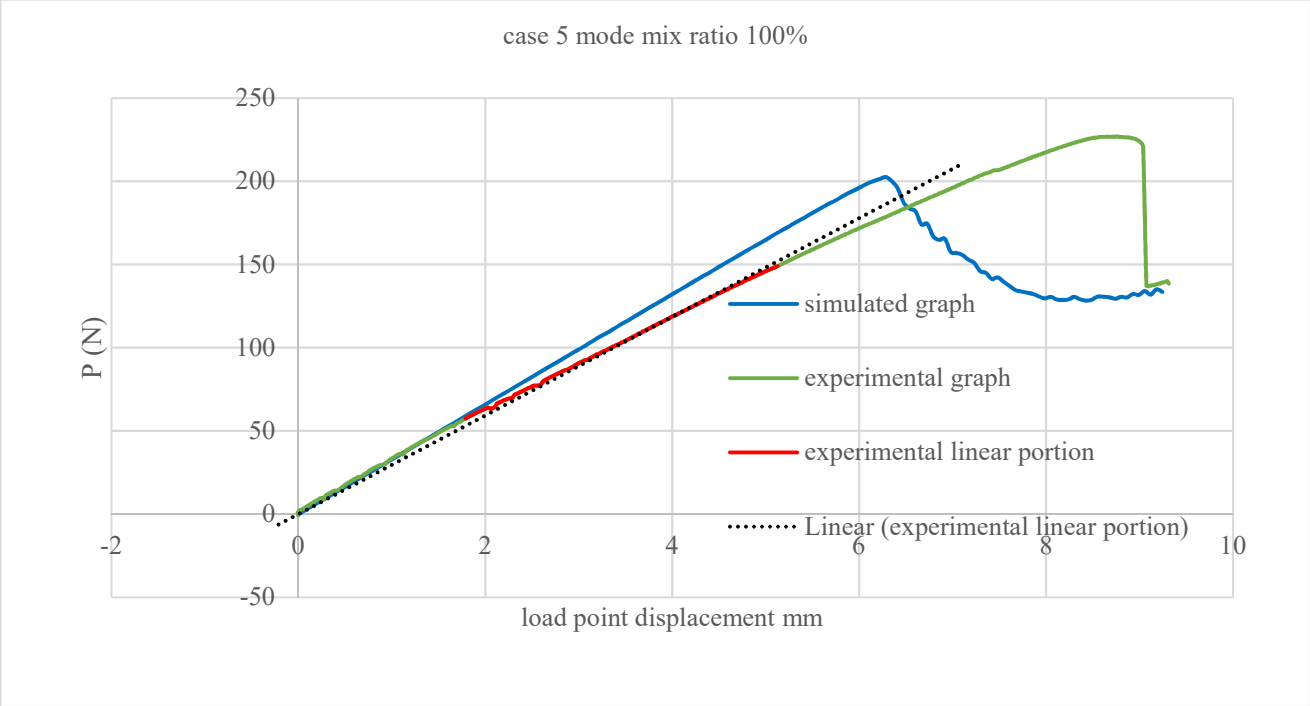

Figure 4. 12 Load displacement graph of case 5

4.6 Conclusions

Validation of numerically simulated model was done with experimental results. Load versus displacement plots were obtained from numerical simulation of the model and were compared with the experimental graphs for all mode mix ratios (20%, 30%, 50%, 75% and 100%). Figure (4.8 to 4.12) shows the graphs of all mode mix ratios.

Load displacement graphs from simulation were compared with linear portion of experimental graphs. Numerical graphs show good agreement with experimental graphs. Graphs overlap each other to the point of progressive damage, from the point of progressive damage percent difference

is high. This difference is due to the mode mix measured from experimental fracture toughness and numerically from progressive B-K criteria.

With the increase of mode mix ratio from 20% to 100%, load P increases, since interlaminar shear toughness is greater than normal out of plane toughness in mode II. With increase of load, load point displacement decreases for high mode mix ratios.

Simulations with mass scaling to speed up the simulation showed that mass scaling to 1×10^{-6} and lower values give results in good agreement, mass scaling higher than this value gives ripples in the solution.

Simulation with different displacement rates showed that it is independent of displacement rates at normal rates. The solution was found in good agreement at 6mm/s.

Chapter 5:

E XAMPLE APPLICATION AND FUTURE RECOMMENDATION

5.1 Overview

The validated cohesive zone model that is obtained from comparison of FE results with experimental results is used to the application of bonded joints.

Bonded joints have several increased structural applications in recent years, due to their certain advantages over other joining methods. Therefore, improved models with the ability to predict damage initiation and propagation, are required for optimum designing and analysis of bonded joints.

Bonded joints have several geometries i.e. single lap joints, double lap joints, stepped joints and scarf joints. In recent years scarf joint method is used extensively in repairing as well in designing of composites.

In this study focus is on scarf joint. The validated cohesive zone model is used for FE modeling of scarf joint. This model predicts initiation and propagation of damage. Dimension for the scarf joint is taken from D. Tzetzis et al paper [40], who have worked on performance of scarf repairs through experimental testing.

The performance of scarf joint depends on the angle through which scarf joint is bonded. In this study, we have analyzed three joints having different bonded angles. Tensile testing is done through FE simulation on three different cases having different bonded angles and performance of each joint is predicted. Graphs showing failure loads are obtained from the simulation. These failure loads are compared for the three cases to predict angle effects in scarf joints.

5.2 Modeling details of scarf joint

Numerical model is created in Abaqus software. The dimensions of the numerical model are taken from D. Tzetzis et al paper [40].The scarf joint was model with a length 320mm, width 40 mm and

Thickness 4.2mm. Overlap layer is also model on the scarf joint which has thickness of 1.05mm and the length of this overlap layer varies with the bonded angle from one edge of the scarf joint to cover the joint portion. Figure (5.1) shows a general figure of scarf joint. Figure (5.2) shows the schematic of the model specimen.

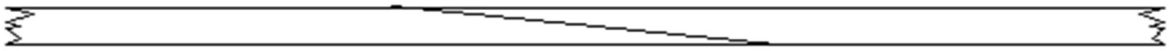

Figure 5. 1 Figure showing scarf joint

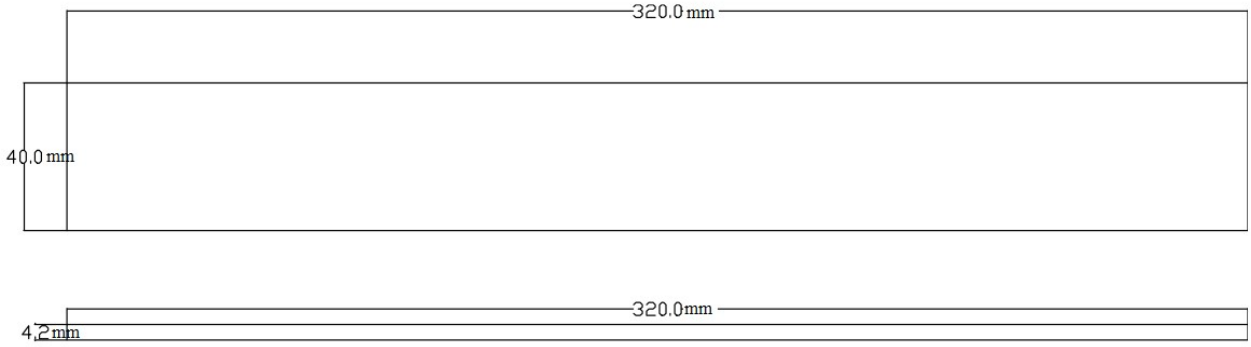

Figure 5. 2 Schematic of scarf joint dimensions

5.2.1 Mesh details

Plies of the specimen are modeled through built-in composite layup of 4 layers with 5th layer as overlap layer and elements used are continuum shell elements with reduced integration (SC8R), Each layer was made of one continuum shell element and was found enough for mesh convergence.

For modeling the joint in the model, interface was inserted in the mid plane at certain angle, specific to the case. This is modeled as cohesive zone elements (COH3D8). The cohesive zone was generated through offset mesh. Increased mesh density is used in specified portion of the specimen,

where the joint area exits which is the focus area in the study as shown in the figure (5.3). As shown from the previous simulations that it is better method for obtaining converged results.

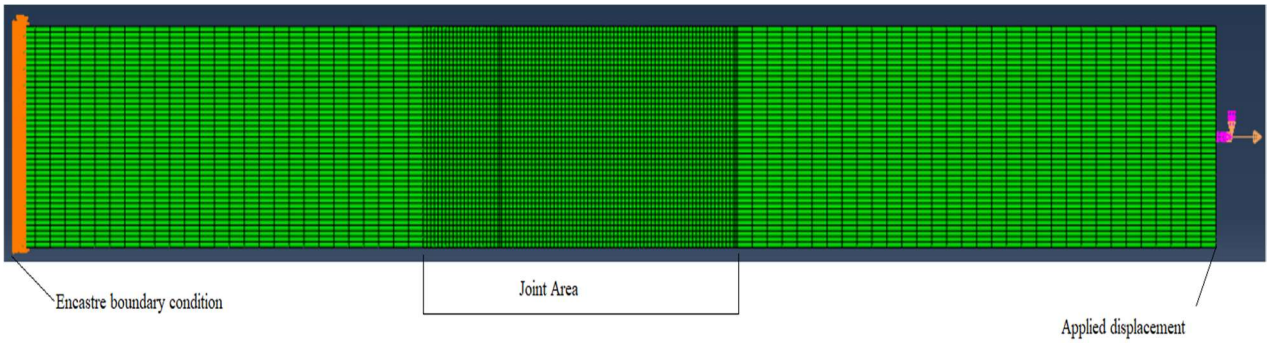

Figure 5. 3 Schematic of mesh details and boundary condition

5.2.2 Boundary Conditions

Figure (5.2) also shows the model boundary conditions. The boundary conditions were set according to a tensile test setup. The model was hinged at one end and load was applied on the other end as applied displacement on a dummy node which was linked to the edge of the specimen.

5.3 Simulations and results

Figure (5.4) shows the comparison of the failure load for the three cases. The graph shows that as the angle decreases that i.e. the length to thickness ratio increases, the failure load increase. So joints with low scarf angles are better for designing purposes.

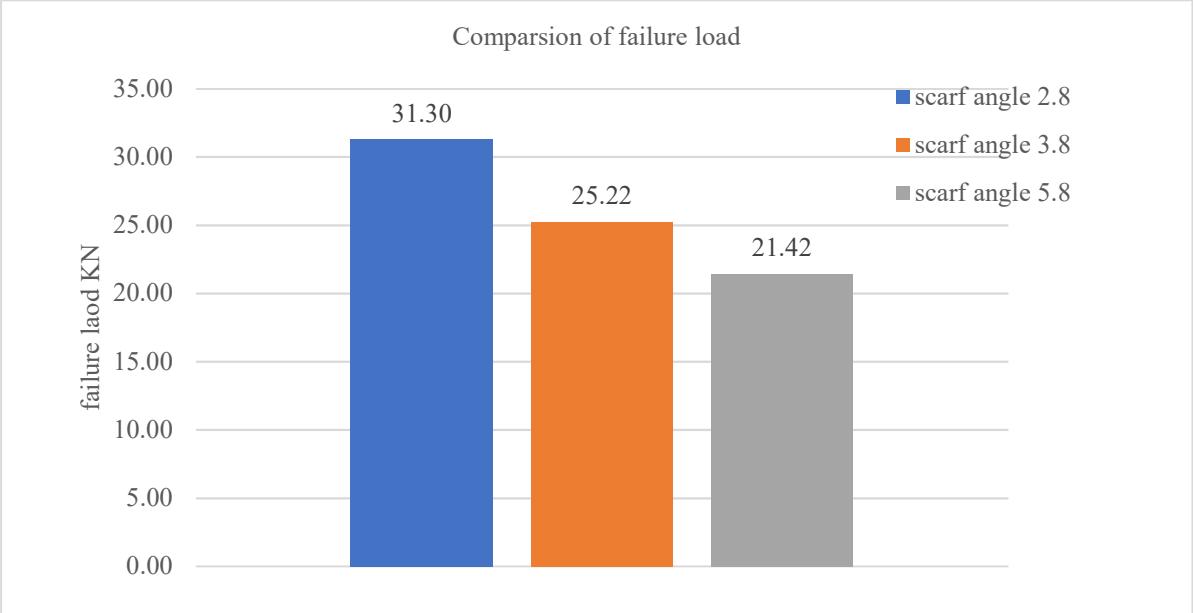

Figure 5. 4 Comparison of failure load

5.4 Future Recommendations

The model can be simulated with adding further details by inserting cohesive layer in each ply and defining damage model for individual ply. Tensile fatigue testing can be done the model. In the application scenario different joint configurations can be compared with each other and other factors effecting the scarf joints can be studied.

References

[1] K. M. Rybicki EF, "A finite element calculation of stress intensity factors by a modified crack closure integral," *Engineering Fracture Mechanics,* vol. 9, p. 931, 1977.

[2] J. R. Rice, "A path independent integral and the approximate analysis of strain concentrations by notches and cracks," *Journal of applied mechanics,* pp. 379-386, 1968.

[3] A. D. H. K. Foulk JW, "Formulation of a three dimensional cohesive zone model for application to a finite elements algorithm.," *Computational Methods and Appllied Mechanical Engineering,* vol. 183, pp. 1-2,51-67, 2000.

[4] D. DS, "Yielding of steel sheets containing slits.," *Nonlinear Dynamics,* vol. 8, pp. 100-4, 1960.

[5] B. L. Allix O, "Mesomodeling of delamination: towards industrial applications," *composite science and technology,* vol. 66, pp. 731-44, 2006.

[6] C. P. C. J. D. C. Turon A, "A damage model for the simulation of delamination under variable-mode loading," *Mechanics of materials,* vol. 38, p. 1072–89, 2006.

[7] B. GI, "The mathematical theory of equilibrium cracks in brittle fracture.," *Advance applied mechanics,* vol. 1962, pp. 55-129, 1962.

[8] M. M. a. P. P. A Hillerborg, " Analysis of crack formation and crack growth in concrete by means of fracture mechanics and finite elements.," *Cement and concrete research,* vol. 6, pp. 773-782, 1976.

[9] J. S. M. B. J. H. a. H. V. P. Naghipour, "Fracture simulation of CFRP laminates in mixed mode bending," *Engineering Fracture Mechanics,* 2009.

[10] G. A. a. M. Crisfield, "Finite element interface models for delamination analysis of laminated composites," *Numerical methods for engineering,* vol. 50, pp. 1701-1736, 2001.

[11] P. P. C. C. G. D. M. F. d. Moura, "Numerical Simulation of Mixed-Mode Progressive Delamination in Composite Materials," *journal of composite materials,* vol. 37, pp. 1414-1424, 2003.

[12] N. S. C. A. J. K. J. G. Williams, "Delamination Fracture of Multidirectional Carbon-Fiber/Epoxy Composites under Mode I, Mode II and Mixed-Mode I/II Loading," *journal of composite materials,* vol. 33, pp. 73-100, 1999.

[13] Y. W. J. W. a. P. Y. A.J. Kinloch, "The mixed-mode delamination of fibre composite materials," *Composites Science and Technology,* vol. 47, pp. 225-237, 1993.

[14] N. a. M. D. Gikhrist, "Mixed-mode delamination of multidirectional carbon fiber/epoxy laminates," *Mechanics of Composite Materials and Structures,* vol. 5, pp. 291-307, 1998.

[15] A. d. M. A.B. Pereira, "Mode I interlaminar fracture of carbon/epoxy multidirectional laminates," *Composites Science and Technology,* vol. 64, pp. 2261-2270, 2004.

[16] A. P. A.B. de Morais, "Mixed mode I + II interlaminar fracture of glass/epoxy multidirectional laminates – Part 1: Analysis," *Composites Science and Technology,* vol. 66, pp. 1889-1895, 2006.

[17] "Standard Test Method for Mixed Mode I-Mode II Interlaminar Fracture Toughness of Unidirectional Fiber Reinforced Polymer Matrix Composites," ASTM, p. D 6671/D 6671M.

[18] D. R. S. Choudhry, "Characterisation and modelling of impact damage in bonded joints of woven fibre polymeric composites," 2009.

[19] P. Naghipour, J. Schneider, M. Bartsch, J. Hausmann, H. Voggenreiter, "Fracture simulation of CFRP laminates in mixed mode bending," *Engineering Fracture Mechanics,* pp. 2821-2833, 2009.

[20] A. Turon, P.P. Camanho, J. Costa, J. Renart, "Accurate simulation of delamination growth under mixed-mode loading using cohesive elements: Definition of interlaminar strengths and elastic stiffness," *Composite Structures,* vol. 92, pp. 1857-1864, 2010.

[21] A. Turon, C.G. Davila, P.P. Camanho, J. Costa, "An engineering solution for mesh size effects in the simulation of delamination using cohesive zone models," *Engineering Fracture Mechanics,* vol. 74, pp. 1665-1682, 2007.

[22] L. Zhao, Y. Gong, J. Zhang,Y. Chen, B. Fei, "Simulation of delamination growth in multidirectional laminates under mode I and mixed mode I/II loadings using cohesive elements," *Composite Structures,* vol. 116, pp. 509-522, 2014.

[23] P.P. Camanho, C.G. Davila, M.F. De Moura, "Numerical Simulation of Mixed-mode Progressive Delamination in Composite Materials," *Composite Materials,* vol. 37, pp. 1415-1438, 2003.

[24] N.E. Jansson, R. Larsson , "A damage model for simulation of mixed-mode delamination growth," *Composite Structures,* vol. 53, pp. 409-417, 2001.

[25] M.L. Benzeggagh, M. Kenane, "Measurement of mixed-mode delamination fracture toughness of unidirectional Glass/Epoxy composites with mixed-mode bending apparatus," *Composite Science and Technology,* vol. 56, pp. 439-449, 1996.

[26] S. Bennati, P. Fisicaro, P.S. Valvo, "An enhanced beam-theory model of the mixed-mode bending (MMB) test—Part I: Literature review and mechanical model," *Meccanica,* vol. 48, pp. 443-462, 2013.

[27] M. Samimi, J.A.W. van Dommelen, M. Kolluri, J.P.M Hoefnagels, M.G.D. Gears, "Simulation of interlaminar damage in mixed-mode bending tests using large deformation self-adaptive cohesive zones," *Engineering Fracture Mechanics,* vol. 109, pp. 387-402, 2012.

[28] A.E. Oskui, N. Choupani and M. Shameli, "3D Characterization of Mixed-Mode Fracture Toughness of Materials Using a New Loading Device," *Latin American Journal of solid and Structures,* vol. 13, 2016.

[29] C. Balzani, W. Wagner, "An interface element for the simulation of delamination in unidirectional fiber-reinforced composite laminates," *Engineering Fracture Mechanics,* vol. 75, pp. 2579-2615, 2008.

[30] A.B. Pereira, A.B. de Morais, A.T. Marques, P.T. de Castro, "Mode II interlaminar fracture of carbon/epoxy multidirectional laminates," *Composite Science and Technology,* vol. 64, pp. 1653-1659, 2004.

[31] M.M. Shokerieh, P.H.M. Attar, "A New Method for Modeling of Initiation and Propagation of Delamination Between [0/θ] of Laminated Composites," *Applied Composite Materials,* vol. 17, pp. 441-452, 2010.

[32] P.W. Harper, L. Sun, S.R hallet, "A STUDY ON THE INFLUENCE OF COHESIVE ZONE INTERFACE ELEMENT STRENGTH PARAMETERS ON MIXED MODE BEHAVIOR," *Applied Science and Manufacturing,* vol. 43, pp. 722-734, 2012.

[33] B. R. K. Blackman, H. Hadavinia, A.J. Kinloch, J.G. Williams, "The use of a cohesive zone model to study the fracture of fibre composites and adhesively-bonded joints," *Fracture,* vol. 119, pp. 25-46, 2003.

[34] R.S. Choudhry, "Characterisation and modelling of impact damage in bonded joints of woven fibre polymeric composites," 2009.

[35] ASTM, "Standard Test Method for Mixed Mode I-Mode II Interlaminar Fracture Toughness of Unidirectional Fiber Reinforced Polymer Matrix Composites," in *ASTM Standards*, ASTM, p. D 6671/D 6671M.

[36] J. a. J. R. Crews, "A mixed-mode bending apparatus for delamination testing," NASA TM 1000662, 1988.

[37] J. a. J. C. Reeder, "Mixed-mode bending method for delamination testing," *AIAA Journal,* vol. 28, pp. 1270-1276. , 1990 .

[38] Abaqus User subroutine manual (v 6.10-1), "V UMAT-User subroutine to define material behaviour section 1.2.17," Abaqus.Inc, 2010.

[39] Cohesive elements section 29.5, "Abaqus Analysis user's manual (v6.10.1)," Abaqus Inc, 2010.

[40] D. Tzetzis, P.J. Hogg, "Experimental and finite element analysis on the performance of vacuum-assisted resin infused single scarf repairs," *Materails and Design,* vol. 29, pp. 436-449, 2008.

Modeling of Delamination Failure in Woven Fabric Reinforced Composites Under Mixed Mode Loading

ORIGINALITY REPORT

8%	4%	5%	1%
SIMILARITY INDEX	INTERNET SOURCES	PUBLICATIONS	STUDENT PAPERS

PRIMARY SOURCES

1	documents.mx Internet Source	1%
2	Choudhry, R.S., Syed F. Hassan, S. Li, and R. Day. "Damage in single lap joints of woven fabric reinforced polymeric composites subjected to transverse impact loading", International Journal of Impact Engineering, 2015. Publication	1%
3	Naghipour, P.. "Fracture simulation of CFRP laminates in mixed mode bending", Engineering Fracture Mechanics, 200912 Publication	1%
4	Harper, P.W.. "A study on the influence of cohesive zone interface element strength parameters on mixed mode behaviour", Composites Part A, 201204 Publication	<1%
5	Zhao, Libin, Yu Gong, Jianyu Zhang, Yuli Chen,	

	and Binjun Fei. "Simulation of delamination growth in multidirectional laminates under mode I and mixed mode I/II loadings using cohesive elements", Composite Structures, 2014. Publication	<1%
6	Submitted to University of Bedfordshire Student Paper	<1%
7	rd.springer.com Internet Source	<1%
8	Mahmood M. Shokrieh. "A New Method for Modeling of Initiation and Propagation of Delamination Between [0/θo] Layers of Laminated Composites", Applied Composite Materials, 04/13/2010 Publication	<1%
9	www.aitdspace.gr Internet Source	<1%
10	qspace.library.queensu.ca Internet Source	<1%
11	dspace.lib.cranfield.ac.uk Internet Source	<1%
12	open.uct.ac.za Internet Source	<1%
13	Bennati, Stefano, Paolo Fisicaro, and Paolo S.	<1%

Valvo. "An enhanced beam-theory model of the mixed-mode bending (MMB) test—Part II: Applications and results", Meccanica, 2013.
Publication

14	Submitted to London School of Marketing Student Paper	<1%

15	Smart Intelligent Aircraft Structures (SARISTU), 2016. Publication	<1%

16	Choupani, N.. "Mixed-mode cohesive fracture of adhesive joints: Experimental and numerical studies", Engineering Fracture Mechanics, 200810 Publication	<1%

17	Maimi', P.. "Matrix cracking and delamination in laminated composites. Part I: Ply constitutive law, first ply failure and onset of delamination", Mechanics of Materials, 201104 Publication	<1%

18	Samimi, M., J.A.W. van Dommelen, M. Kolluri, J.P.M. Hoefnagels, and M.G.D. Geers. "Simulation of interlaminar damage in mixed-mode bending tests using large deformation self-adaptive cohesive zones", Engineering Fracture Mechanics, 2012. Publication	<1%

---

boltonpestcontrol.info

19	Internet Source	<1%
20	www.feastsoftware.com Internet Source	<1%
21	www.deepdyve.com Internet Source	<1%
22	de Moura, M.F.S.F., J.P.M. Gonçalves, and F.G.A. Silva. "A new energy based mixed-mode cohesive zone model", International Journal of Solids and Structures, 2016. Publication	<1%
23	www.wmt.com Internet Source	<1%
24	Cui, Hao. "Simulation of ductile adhesive failure with experimentally determined cohesive law", Composites Part B Engineering, 2016. Publication	<1%
25	Li, Cunbao Xie, Lingzhi Ren, Li Xie, Hep. "Evaluating the applicability of fracture criteria to predict the crack evolution path of dolomite ba", Mathematical Problems in Engineering, Annual 2014 Issue Publication	<1%
26	Samit Roy, Abhishek Kumar. "Effect of particle size on mixed-mode fracture of nanographene	<1%

reinforced epoxy and mode I delamination of its carbon fiber composite", Composite Structures, 2017
Publication

27	www.earthsystemschool.de Internet Source	<1%
28	repository.tudelft.nl Internet Source	<1%
29	Mortensen, F.. "Analysis of adhesive bonded joints: a unified approach", Composites Science and Technology, 200206 Publication	<1%
30	Moslemi, Mohsen, and Mohammadreza Khoshravan azar. "Delamination analysis of woven fabrication laminates using cohesive zone model", Journal of Central South University, 2016. Publication	<1%
31	dc.library.okstate.edu Internet Source	<1%
32	Xue, P.. "A non-orthogonal constitutive model for characterizing woven composites", Composites Part A, 200302 Publication	<1%
33	Jimenez, Stephen, Xia Liu, Ravindra Duddu, and Haim Waisman. "A discrete damage zone	<1%

model for mixed-mode delamination of composites under high-cycle fatigue", International Journal of Fracture, 2014.
Publication

34	Raffaella Magrassi. "Protection capabilities of nanostructured shells toward cell encapsulation: A Saccharomyces/Paramecium model", Microscopy Research and Technique, 2010 Publication	<1%
35	Theresa M. Roeder, Lee W. Schruben. "Information models for queueing system simulation", ACM Transactions on Modeling and Computer Simulation, 2010 Publication	<1%

Exclude quotes	Off	Exclude matches	Off
Exclude bibliography	Off		

CERTIFICATE OF COMPLETENESS

It is hereby certified that the dissertation submitted by NS Jawadullah, Reg No. **NUST201464468MCEME35114F**, Titled: ***Modeling of delamination failure in woven fabric reinforced composites under mixed loading*** has been checked/reviewed and its contents are complete in all respects.

Supervisor's Name: **Dr. Hasan Aftab Saeed** Signature: _____

Date: _____